

G. Sergienko, G. Arnoux, S. Devaux, G.F. Matthews, I. Nunes, V. Riccardo,
A. Sirinelli, A. Huber, S. Brezinsek, J.W. Coenen, Ph. Mertens,
V. Philipps, U. Samm and JET EFDA contributors

Movement of Liquid Beryllium During Melt Events in JET with ITER-Like Wall

Movement of Liquid Beryllium During Melt Events in JET with ITER-Like Wall

G. Sergienko¹, G. Arnoux², S. Devaux³, G.F. Matthews², I. Nunes², V. Riccardo²,
A. Sirinelli², A. Huber¹, S. Brezinsek¹, J.W. Coenen¹, Ph Mertens¹, V. Philipps¹,
U. Samm¹ and JET EFDA contributors*

JET-EFDA, Culham Science Centre, OX14 3DB, Abingdon, UK

¹*Institute of Energy and Climate Research – Plasma Physics, Forschungszentrum Jülich,
EURATOM Association, Trilateral Euregio Cluster, D-52425 Jülich, Germany*

²*EURATOM/CCFE Fusion Association, Culham Science Centre, Oxon OX14 3DB, UK*

³*Max-Planck-Institut für Plasmaphysik, EURATOM-Assoziation, D-85748 Garching, Germany*

** See annex of F. Romanelli et al, “Overview of JET Results”,
(24th IAEA Fusion Energy Conference, San Diego, USA (2012)).*

Preprint of Paper to be submitted for publication in Proceedings of the
14th International Conference on Plasma-Facing Materials and Components for Fusion Applications,
Jülich, Germany.
13th May 2013 - 17th May 2013

“This document is intended for publication in the open literature. It is made available on the understanding that it may not be further circulated and extracts or references may not be published prior to publication of the original when applicable, or without the consent of the Publications Officer, EFDA, Culham Science Centre, Abingdon, Oxon, OX14 3DB, UK.”

“Enquiries about Copyright and reproduction should be addressed to the Publications Officer, EFDA, Culham Science Centre, Abingdon, Oxon, OX14 3DB, UK.”

The contents of this preprint and all other JET EFDA Preprints and Conference Papers are available to view online free at www.iop.org/Jet. This site has full search facilities and e-mail alert options. The diagrams contained within the PDFs on this site are hyperlinked from the year 1996 onwards.

ABSTRACT.

The ITER-Like Wall recently installed in JET comprises solid beryllium limiters and a combination of bulk tungsten and tungsten-coated carbon fibre composite divertor tiles without active cooling. During a beryllium power handling qualification experiment performed in limiter configuration with 5MW NBI input power, accidental beryllium melt events, melt layer motion and splashing were observed locally on few beryllium limiters at the plasma contact areas. The Lorentz force is responsible for the observed melt layer movement. To move liquid beryllium against the gravity force, the current flowing from the plasma perpendicularly to the limiter surface must be higher than 6kA/m^2 . The thermo-emission current at the melting point of beryllium is much lower. The upward motion of the liquid beryllium against gravity can be due to a combination of the Lorentz force from the secondary electron emission and plasma pressure force.

1. INTRODUCTION

Beryllium, a low Z metal, is selected as a plasma-facing material for the first wall armour in ITER [1]. In spite of good thermo-mechanical properties giving the capability to handle a few MW/m^2 , beryllium has a low melting point of 1285°C and a high vapour pressure of 5Pa at the melting point. Under melt events, which were observed early in the ISX-B tokamak – one of the first experiments with beryllium limiters [2] – liquid beryllium can be moved by gravity, surface tension, plasma pressure and Lorentz forces acting conjointly. The liquid metal motion causes an enhanced erosion of the wall component and can reduce the power handling capability because shape alteration leads to hot spot formation. Melting events were also observed on JET in earlier experiments with beryllium tiles [3]. The ITER-Like Wall (ILW) recently installed in JET comprises solid beryllium limiters with a power handling of $4 - 6\text{MW/m}^2$ and a combination of bulk tungsten and tungsten-coated carbon fibre composite divertor tiles without active cooling [4]. JET ILW provides a unique opportunity to study beryllium power handling at its limit to gain an experience with beryllium melt events, which is necessary for controllable operation of future fusion devices.

2. EXPERIMENTAL

A beryllium power handling experiment [5] performed in limiter configuration with 5MW NBI input power over 10s was carried in JET in order to verify the design values of the poloidal limiters [6,7]. The beryllium poloidal limiters with inertial cooling should be capable of withstanding the power flux of 6MW/m^2 during 10s without melting for a starting base temperature below 400°C [7]. The plasma configurations with plasma limited either by 10 inner guard wall limiters (IGWL) or by 8 wide outer poloidal limiters (WOPL). Power fluxes to the 8Z beryllium limiter (one of the IGWL located in octant 8 of the JET torus) were measured with help of the near infrared ($\lambda = 3.99\ \mu\text{m}$) camera [8]. To increase power flux onto the IGWL, the plasma in the Pulse No: 83620 (the evolution of plasma parameters of the discharge shown in figure 1) was positioned slightly above the mid-plane as shown in figure 2 that reduced a plasma contact area due to a poloidal

shape of the IGWL. The maximum surface temperature and power flux to the 8Z limiter reached respectively $\approx 980^\circ\text{C}$ and $\approx 3\text{MW}/\text{m}^2$. Unexpectedly, at about 12.3s, the plasma radiation power started to increase periodically. The plasma radiation bursts correlated with sawtooth oscillations and was accompanied by a periodical increase of the beryllium (mainly *Be II* (467nm) line) emission on the top of 8Z and adjacent 8X beryllium limiters measured by means of the wide view CCD colour camera (the blue frame was only used) as seen in figure 1. Z_{eff} was also slightly increased from 1.7 to 2 during these events, which points out almost 50% increase of the beryllium density in the plasma. The wide view near infrared ($\lambda = 1 \mu\text{m}$) CCD camera used for the wall protection [9] detected a hot spot at the plasma contact area on the 8X limiter with a temperature above 1150°C . Images of the near infrared CCD camera showed the appearance of the local volumetric emission near 8X limiter during spikes of *Be II* line emission. These events lasted about 1s until a plasma disruption occurred at 13.5 s, which was caused by mode-locking. Visual inspection with the help of an in-vessel video inspection system performed after this experiment showed significant local melting on the apex of several beryllium limiters, both IGWL and WOPL. High resolution images of all limiters were taken at the start of the shutdown for JET maintenance. The melting areas of 4X and 8X IGWL beryllium limiters are shown in figure 3. The melting areas of upper part 6D and mid part 7B WOPL beryllium limiters are shown in figure 4. The major melting areas are on the tangential limiter surfaces where the magnetic last closed flux surface (LCFS) touches the limiter apex. The traces of the beryllium jets originated from major melt regions are well seen on these high resolution images. Molten beryllium moved upwards on IGWL and moved downwards on WOPL. The liquid beryllium travelled over significant distances on IGWL passing across the 0.35mm castellation and 2–3mm tile gaps, sometimes jumping over a distance of about 2 cm. The jet propagation angles were 7.5° , 10.5° – 17° and 14° , 21.5° , 23.7° with respect to the IWGL and WOPL beam vertical axis respectively. To summarise, the melting certainly occurred in the Pulse No: 83620 for displayed IGWL and this melting was accompanied with periodical fast melt layer motion and beryllium droplet injections into the plasma. The melting of the WOPL presumably happened, during discharge #83610 with the plasma limited on the low field side when the highest temperature on the 7D limiter was reached around 1100°C and the discharge was stopped by the wall protection system indicating too much power hitting the wall element. No evidence of melting on Z_{eff} or plasma radiation was observed in this plasma discharge, therefore, there is probably no beryllium droplet injection into the plasma in this discharge. Unfortunately, there is no direct observation of the WOPL 6D limiter.

3. DISCUSSION

The upwards motion of liquid beryllium on the high field side limiters and downwards motion on the low field side limiters confirms the action of the Lorentz force and that the electrical currents flow from the plasma to the beryllium surface. One can estimate the required minimum value of this current so that the gravity force is compensated by the Lorentz force. Taking into account

that the local toroidal magnetic field was $B_t = 2.73\text{T}$ and the density of beryllium at the melting point temperature is $\rho = 1690\text{kg/m}^3$ [10], we get $j_{\perp} > \rho g/B_t = 6\text{kA/m}^2$. To define this current more accurately the traces of liquid beryllium jets on the limiter shown in figures 3 and 4 should be taken into account. The direction of liquid beryllium motion is defined by the direction of the net force due to the combined action of gravity force, Lorentz force and force induced by the plasma pressure. The force diagram is shown on figure 3 for the high field side and on figure 4 for the low field side. Taking into account that the angle between magnetic field lines and limiter surface is about of 5° , the propagation angle of a melt layer with thickness 1mm was calculated as a function of current density normal to the limiter surface and plasma pressure. The result of these calculations for IGWL and WOPL is shown in figure 5. The maximum power density at the melt areas of IGWL reached 5MW/m^2 probably due to small toroidal misalignment of the limiters or tile-to-tile misalignment. Taking into account that the plasma pressure estimated from the maximum heat flux density was about of 150–200Pa and the range of observed propagation angles of beryllium jets, one can find that the maximum possible current density normal to the melt layer surface should be below 70kA/m^2 . The estimated current range of 6–70 kA/m^2 is comparable with the ion saturation current to the surface. In the case of molten tungsten this current is the result of thermo-electron emission [11], which is strong enough (about 1MA/m^2) to move liquid tungsten against gravity forces in the edge plasma when the magnetic field is higher than 0.15 T. The beryllium melts at much lower temperature and the thermo-electron emission current is very small at the melting point of beryllium. The Lorentz force exceeds the gravity force only at temperatures about 100K below the boiling point of beryllium, as seen on figure 6. The beryllium oxide has a higher thermo-electron emission but it is unlikely to be present on the beryllium surface exposed to the high deuterium plasma flux. In addition, the thermo-electron current from BeO would still be too small at the melting point of beryllium. Therefore, one can conclude that thermo-electron emission is not sufficient to explain the observed motion of the liquid beryllium. The limiter surfaces close to the LCFS collect plasma electrons and the total current should be directed from the surface to the plasma. Thus, the plasma halo currents cannot be responsible for this motion either. The observed liquid beryllium motion can be caused by currents due to the secondary electron emission. Similar liquid metal (stainless-steel) motion was observed in [12] and also can be explained by the secondary emission currents. The effective secondary electron coefficient of plasma face materials close or above 1 was often observed in the scrape-off layer plasma of tokamaks [13, 14]. The secondary electron emission depends on the electron plasma temperature, magnetic field line inclination angle to the surface and sheath potential. In the case of the magnetic field line normal to the surface, effective secondary emission from beryllium exceeds 1 if the electron temperatures lie above 40eV [15]. The effective secondary electron emission coefficient reduces with angle between magnetic field and surface because the emitted secondary electrons promptly return to the surface due to their gyro-motions. The increase of the sheath potential also increases the probability to escape from the surface for the low energy secondary electrons due to the acceleration and drift in the sheath. As a result the

effective secondary emission at electron temperature $T_e=100$ eV varies in the range 0.07–0.7 when sheath potential changes from 0 to $-2.84 T_e$ [16]. For the upper values of the sheath potential, the secondary emission current is comparable to the ion saturation current and strong enough to move the liquid beryllium against gravity. The electron temperatures increases during sawteeth crashes and, as a consequence, the secondary emission current will increase too, an effect which can explain the observed fast periodical motion of the molten beryllium. In addition, the presence of the impurities with high secondary emission coefficient such as beryllium oxide or nickel beryllide on beryllium surfaces could essentially increase the effective secondary emission coefficient. The observed liquid beryllium jet jumping (on the IWGL 4X seen on the figure 3) over large distances can be explained by the appearance of the current along the jet when the jet tip loses the electrical contact with a conducting surface. The secondary emission current collected by the jet tip will flow along the jet towards the good electrical contact point to the surface. The Lorentz force due to this longitudinal current pushes the melt jet back to the surface. The larger the detached part of the jet, the higher the longitudinal current and the quicker the jet will reattach back to the surface.

CONCLUSIONS

The thermo-electron emission current from pure beryllium at the melting point is not sufficient to explain the observed motion of liquid beryllium. The plasma halo current cannot explain this motion either because it has the opposite direction. The liquid beryllium motion can be caused by the current due to the secondary electron emission, which is high enough for electron temperature above 40 eV. The current along the liquid metal jet moving on the conducting surface prevents the detachment of the jet from the surface. After the melt damage, beryllium limiters could operate in divertor configuration without degradation of the plasma performance.

ACKNOWLEDGEMENTS

This work was supported by EURATOM and carried out within the framework of the European Fusion Development Agreement. The views and opinions expressed herein do not necessarily reflect those of the European Commission.

REFERENCES

- [1]. H, Barabash V, Federici G, Linke J, Loarte A, Roth J, Sato K, 2002 *Journal of Nuclear Materials*, **307–311** 43–52
- [2]. Mioduszewski P.K, et al. 1986 *Nuclear Fusion*, **26** 1171-1192
- [3]. Loarte A, Saibene G, Sartori R, Campbell D.J, Lomas P.J, Matthews G.F, 2005 *Journal of Nuclear Materials*, **337–339** 816–820
- [4]. Matthews G.F, et al. 2011 *Physica Scripta*, **T145** 014001
- [5]. Arnoux G, et al. this conference
- [6]. Nunes I, de Vries P, Lomas P 2007 *Journal of Fusion Engineering and Design*, **82** 1846–1853

- [7]. Riccardo V, Firdaouss M, Joffrin E, Matthews G, Mertens Ph, Thompson V and Villedieu E 2009 *Physica Scripta*, **T138** 014033
- [8]. Gauthier E, et al. 2007 *Fusion Engineering and Design*, **82** 1335-1340
- [9]. Arnoux G, et al. 2012 *Review of Scientific Instruments* **83** 10D727
- [10]. Cardarelli F, 2008 *Materials Handbook: A Concise Desktop Reference – Second Edition* (New York: Springer)
- [11]. Sergienko G, et al. 2007 *Physica Scripta*, **T128** 81–86
- [12]. Tsuzuki K, et al. 2006 *Fusion Engineering and Design*, **81** 925–929
- [13]. Pitts R.A, and Matthews G F 1990 *Journal of Nuclear Materials*, **176–177** 877-882
- [14]. Gunn J.P, 2012 *Plasma Physics and Controlled Fusion*, **54** 085007
- [15]. Smirnov R D, Krasheninnikov S.I, and Pigarov A Yu, 2009 *Physics of Plasmas*, **16** 122501
- [16]. Nishimura K, Kawata J, Ohya K, 1996 *Journal of Plasma and Fusion Research*, **72** 535-541

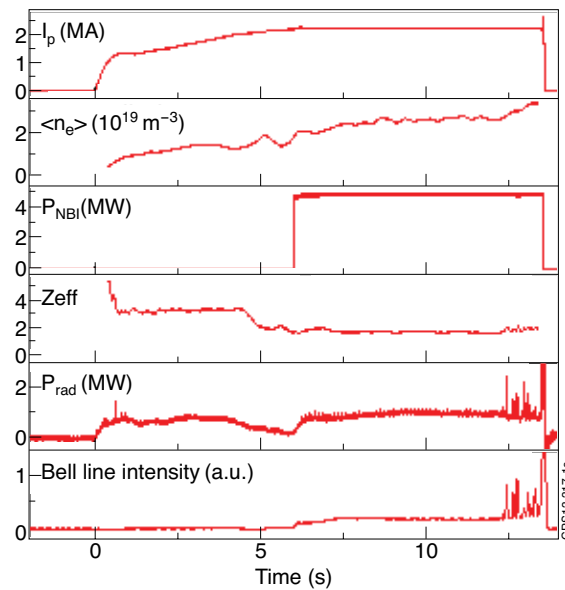


Figure 1: Time evolution of plasma current I_p , line averaged electron density $\langle n_e \rangle$, effective plasma charge Z_{eff} , radiated power P_{rad} and beryllium (mainly Be II (467nm)) line intensity for the Pulse No: 83620.

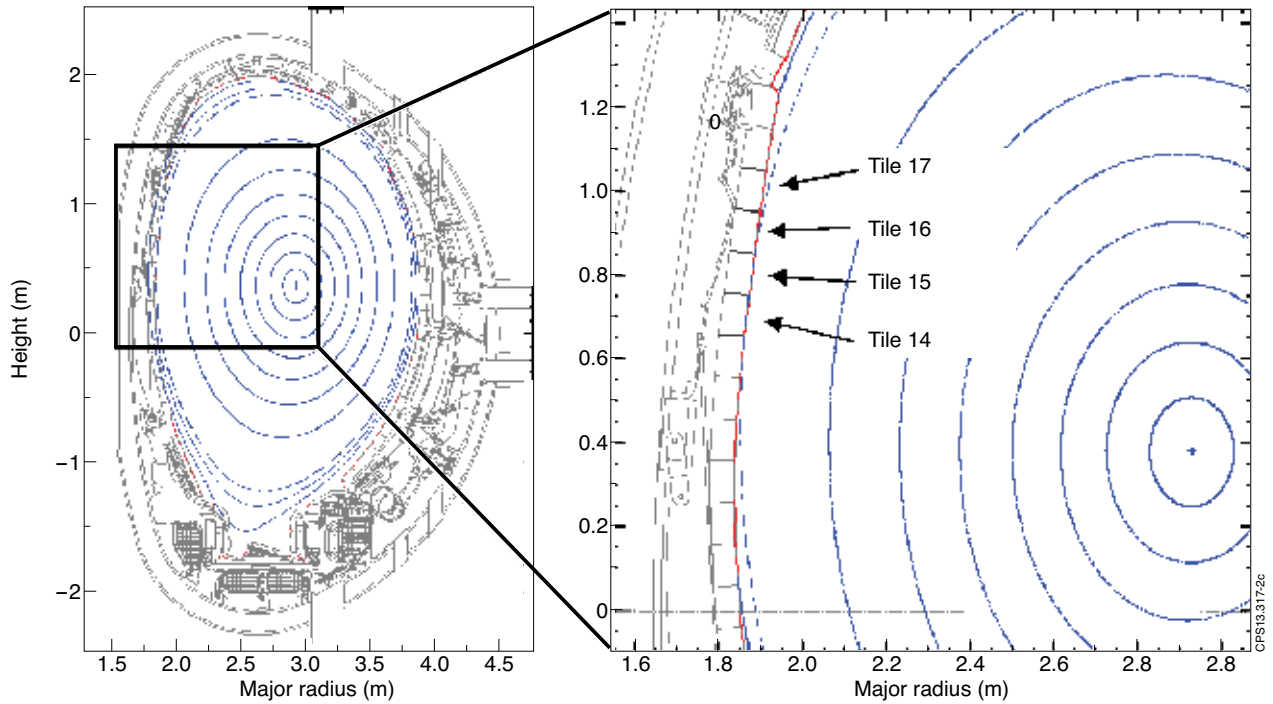


Figure 2: Magnetic fields configuration, Pulse No: 83620 $t = 13.3s$.

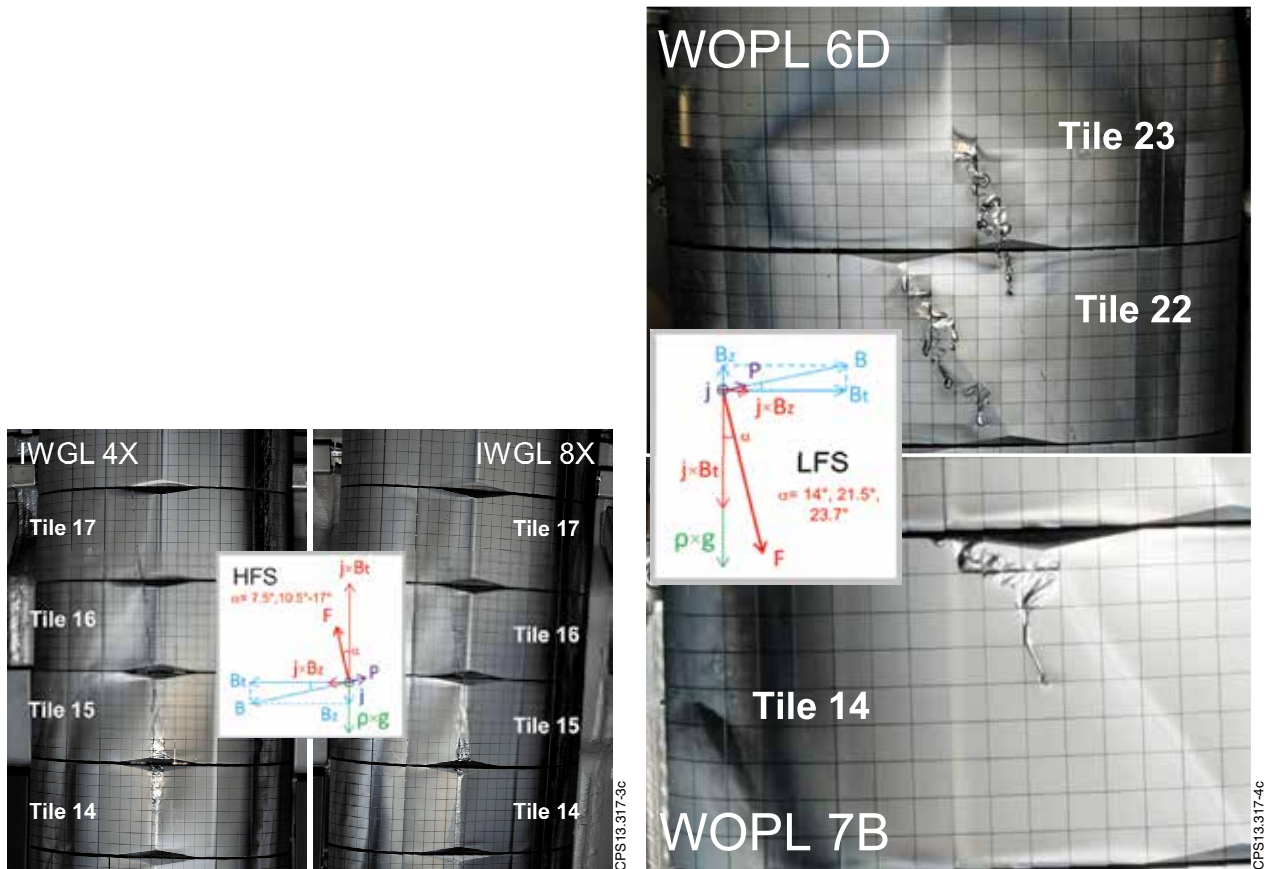


Figure 3: Molten 4X and 8X IWGL (inner wall guard limiters).

Figure 4: Molten 6D and 7B WOPL (wide outer poloidal limiters).

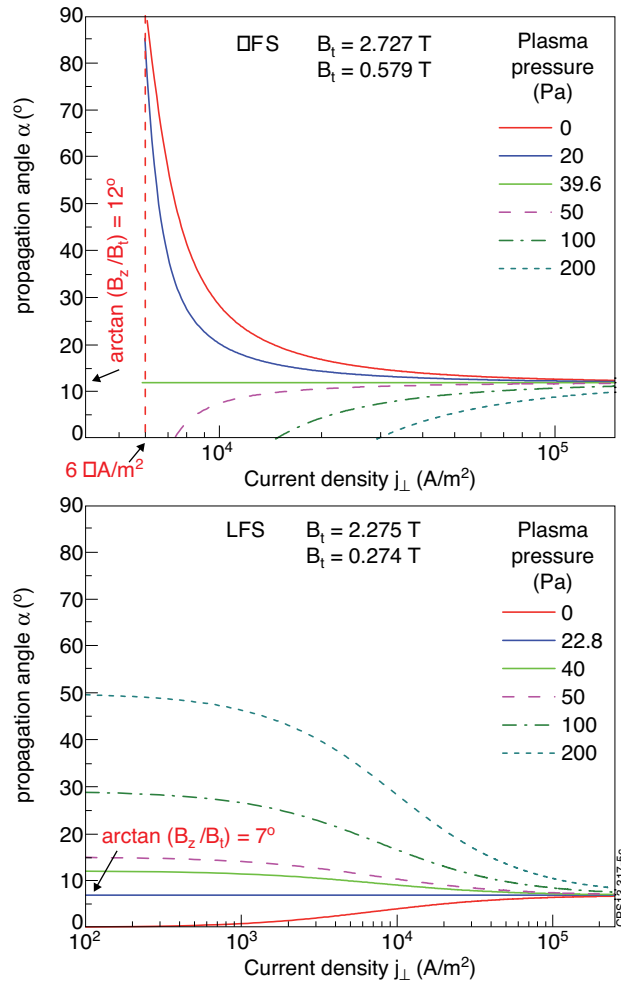


Figure 6: Calculated thermo-electron current for Be and BeO as a function of surface temperature.

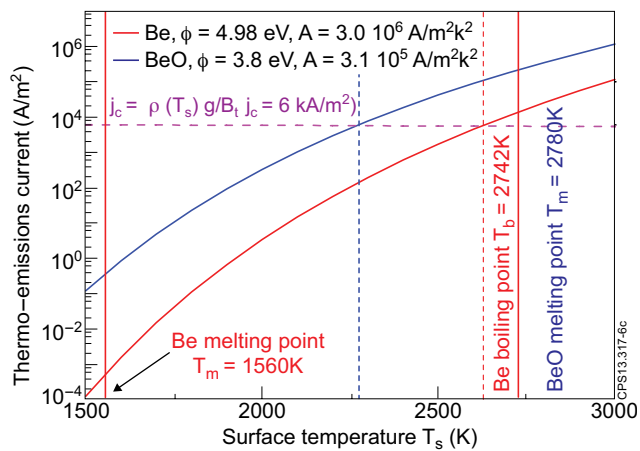


Figure 5: Calculated propagation angle of 1mm thick melt layer as a function of the current density to the surface and of the plasma pressure.